MDPI

Comparative Analysis of Tunnel Plastic Zone Calculation and Engineering Measurement Based on Various Methods

Zhihong Dong [1,2], **Qingwen Yan** [3], **Qifeng Guo** [1,2,*], **Xun Xi** [1,2], **Xianquan Lei** [4] **and Wenhui Tan** [1,2,*]

1   School of Civil and Resource Engineering, University of Science and Technology Beijing, Beijing 100083, China
2   Key Laboratory of High-Efficient Mine and Safety of Metal Mines, University of Science and Technology Beijing, Beijing 100083, China
3   Huize Mining Company, Yunnan Chihong Zinc and Germanium Co., Ltd., Qujing 654200, China
4   CINF Engineering Co., Ltd., Changsha 410019, China
*   Correspondence: guoqifeng@ustb.edu.cn (Q.G.); wenhui.t@163.com (W.T.)

Abstract: The characteristics of plastic zone are a critical basis for the control and stability analysis of the surrounding rock of roadways. This paper aims to investigate the rationality and applicability of the numerical methods for the plastic zone analysis of deep jointed rock roadways. Based on the detailed investigation and experiments, The plastic zone distribution of roadway surrounding rock under different GSI values and different buried depths was analyzed by analytical methods, parameter reduction, and equivalent rock mass technology, and then the acoustic wave measurement method was used to carry out the field measurement and was compared with the simulation results. The results show that when GSI is large, the difference between the results is not obvious. When GSI is small, the results obtained by the parameter reduction method and the analytical method show a more drastic increase and the discreteness increases. The results obtained by the equivalent rock mass technique are generally close to the measured values, and the growth rate is more uniform. According to the convenience of the calculation parameters and the accuracy of the calculation, the suitable calculation methods for different working conditions were suggested.

1. Introduction

The volume and distribution of surrounding rock plastic zone are important parameters for roadway stability analysis, support and reinforcement design, monitoring, and early warning of surrounding rock safety control technology. In engineering, the physical detection method is often used to conduct field measurement of surrounding loose rock zone. Zhang et al. [1] used rock mass ultrasonic detection and a digital panoramic drilling camera to obtain the range of surrounding rock loosening zone in deep roadway. Xu Kun et al. [2] used the single-hole acoustic test method to test the depth of the fracture zone of the surrounding rock. Jing Hongwen et al. [3] took the circularity of cracks measured from borehole images as the criterion for judging surrounding rock loosening zone. Guo Liang et al. [4] measured the range of loose circle by GPR. However, the operation of field measurement of surrounding rock plastic zone is difficult and is easily limited by field environment and construction conditions, and the cost is high, so it is impossible to give prediction guidance before roadway excavation.

Analytical methods based on rock elastic-plastic theory and damage theory can well explain the formation and evolution mechanism of surrounding rock [5–9]. However, when the rock section is complex, it is difficult to obtain an accurate analytical solution. At the same time, there are structural planes of different sizes in rock mass, so it is difficult for the theoretical analysis method to consider the real weak plane of rock mass structure. At the same time, there are structural planes of different sizes in rock mass, so it is difficult

for the theoretical analysis method to consider the real weak plane of rock mass structure. The numerical simulation method can efficiently solve the plastic zone distribution of surrounding rock, solve the complex section and engineering geology problems, and has been more widely used. Xiao Ming et al. [10] determined the range of surrounding rock loosening zone under excavation blasting through numerical calculation. Zhou Zhihua [11] used ANSYS software to establish a model to simulate the loose zone of surrounding rock of soft rock roadway and identified the distribution of plastic zone of roadway through the stress distribution characteristics of roadway. Xiong Liangxiao et al. [12] used FLAC3D to analyze the stress path and the change process of safety factor caused by deep tunnel excavation and also made certain research achievements in dynamic damage and environmental impact [13,14]. However, most studies regard surrounding rock as homogenate, but from the actual situation, roadway surrounding rock is usually anisotropic and discontinuous, composed of discontinuous surface and structure. The existence of discontinuities makes the rock mass appear as a collection of broken blocks, which reduces the stability of the rock mass [15–17]. Compared with the intact rock, various parameters of the jointed rock mass can be obtained through reduction or equivalent calculation and then simulated and analyzed. Hoek-Brown [18] criterion is widely used as a commonly used method for rock mass parameter reduction. Massimiliano Fraldi et al. [19–21] compared the differences between different calculation methods based on limit analysis approaches when the plastic zone is calculated and proposed a straight characterization, which can help to evaluate the risk of a tunnel collapse with respect to the depth of excavation. Wu Shunchuan et al. [22] proposed equivalent proximity and compared and analyzed the rationality of various reduction paths. Hu Mingsheng et al. [23] comprehensively considered the characteristics of the structural plane and the number of joint volumes and used the Hoek-Brown criterion to reduce the rock mass parameters after classifying the rock mass based on the GSI system. Su Yonghua et al. [24] tracked the progress of the methods adopted by Hoek-Brown criterion to estimate the mechanical parameters of rock mass by using the mechanical parameters of rock blocks and various improvement measures.

Equivalent rock mass technology is a reliable mean of numerical calculation in terms of large-scale rock mass stability analysis in recent years. The method by adding discrete fracture network (DFN) numerical model to build realistic rock joints and fissures distribution model, and the calculation results compared with the calculation model and homogenization of continuous medium joint calculation model is more reliable. Wu Shunchuan et al. [25–27] constructed an equivalent rock mass model that could fully reflect the distribution characteristics of engineering rock mass joints and verified the suitability and reliability of equivalent rock mass technology in the study of mechanical properties of discontinuous jointed rock masses. Zhu Wancheng et al. [28–30] conducted numerical simulation tests on equivalent rock mass to determine the rock mass characterization element and then studied the mechanical properties of engineering scale rock mass.

In engineering, when different rock mass parameters of different quality levels are converted by different methods, the difficulty of obtaining various basic properties and necessary parameters is different. The applicability, difference, and accuracy of parameter reduction method and equivalent rock mass technique in plastic zone analysis for different grades of surrounding rock and in situ stress conditions are still unclear. Relying on a mine in Yunnan province, this paper is based on the detailed engineering geological investigation, rock mechanics test, in situ stress test, equivalent rock mass parameters, which were used respectively to fold the subtraction and technical analysis of the plastic zone of surrounding rock, programming to extract the plastic zone size calculation, using the method of acoustic measurement of roadway surrounding rock loose circle of field measurement analysis, comparing simulation and the measured results, comparing the difference between the two numerical methods, and the applicability of the two methods to calculate the plastic zone under different surrounding rock grades and depths is also analyzed.

2. Analysis of Plastic Zone of Roadway

2.1. Analytical Solution Analysis of Plastic Zone in Roadway Surrounding Rock

According to the existing research results [31,32], based on the plane strain mechanical model of circular holes shown in Figure 1, the implicit equation of plastic zone boundary of non-isobaric circular roadway surrounding rock with respect to r, θ is obtained.

$$
\begin{aligned}
f(r,\theta) = & \left\{ (P+\lambda P)(R_0^2/r^2) - \cos 2\theta(\lambda P - P)[1 + 3(R_0^2/r^2)^2 - 2(R_0^2/r^2)] \right\}^2 + \\
& \left\{ \sin 2\theta(\lambda P - P)[1 - 3(R_0^2/r^2)^2 + 2(R_0^2/r^2)] \right\}^2 - \\
& \left\{ [(P+\lambda P) - 2\cos 2\theta(\lambda P - P)(R_0^2/r^2)]^2 - 4c^2 \right\} \frac{(1-\cos 2\varphi)}{2} - \\
& 4c^2 - 2c\sin 2\varphi[(P+\lambda P) - 2\cos 2\theta(\lambda P - P)(R_0^2/r^2)]
\end{aligned}
\tag{1}
$$

where r and θ are the polar coordinates of any point on the boundary of plastic zone of roadway surrounding rock; P is vertical principal stress; R_0 is the roadway radius; λ is the lateral pressure coefficient; c is the cohesion of surrounding rock; and φ is the friction angle in the surrounding rock. This method is abbreviated as AN in the following.
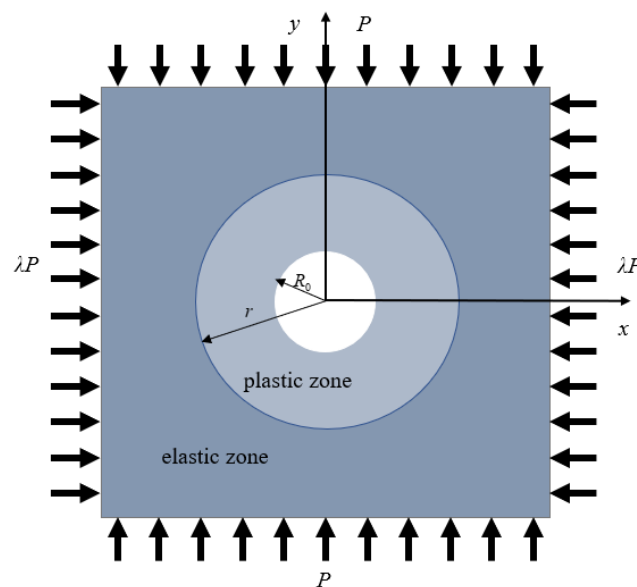

Figure 1. Circular roadway surrounding rock force model in the inhomogeneous stress field.

2.2. Analysis of Plastic Zone of Roadway Based on Parameter Reduction Method

Hoek-Brown criterion is widely used in slope engineering, tunnel chamber, and hydraulic engineering to calculate the rock mass parameters. The GSI value of roadway surrounding rock is obtained through joint and fracture investigation, combined with complete rock physical and mechanical parameters, and according to the latest Hoek-Brown criterion [18], the strength parameters of rock mass under different quality levels can be calculated, as shown in the Figure 2. And then the reduced relevant parameters are assigned to the numerical model for calculation, and the settlement result of roadway plastic zone can be obtained. This method is abbreviated as RE in the following.
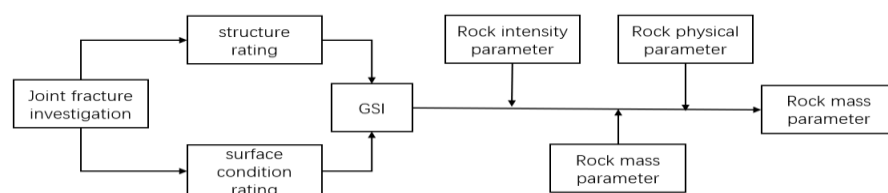

Figure 2. Process of parameter reduction method to obtain rock mass parameters.

2.3. Analysis of Plastic Zone of Roadway Based on Equivalent Rock Mass Technology

By combing discrete fracture network (DFN) with discrete element numerical software (3DEC, PFC, etc.), the equivalent rock mass model is formed by block model, particle model, and smooth joint model, as shown in the Figure 3. In this paper, a calculation model close to the real rock mass is constructed by combining 3DEC and DFN models, which can be obtained based on the joint structure information of roadway surrounding rock. Through the smooth joint model, the parameters, such as joint density, trace length, and occurrence information, can be more truly reflected in the calculation model. Combined with different boundary conditions and mechanical properties of intact rock, the plastic zone of the roadway of jointed rock mass under different working conditions can be calculated and analyzed. This method is abbreviated as EQ in the following.
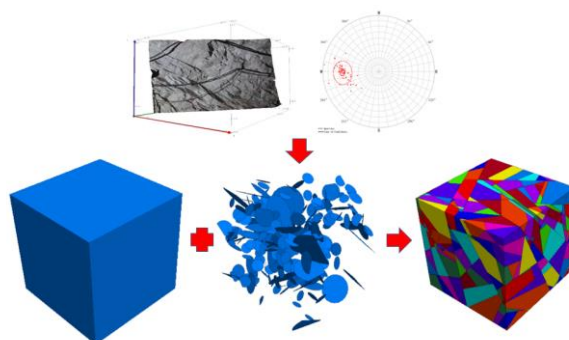

Figure 3. Main process of equivalent rock mass technology.

3. Calculation Parameter Acquisition of Plastic Zone of Jointed Rock Mass Roadway

3.1. Determination of Mechanical Properties of Surrounding Rock Foundation in Deep Roadway

The rock mechanics experiments of uniaxial compression deformation, Brazilian splitting, and variable angle shear were carried out after the rock samples were processed. The basic parameters obtained from the rock mechanics experiments are as shown in the Table 1.

Table 1. Mechanical properties of rocks at different depths.

Depth/m	Uniaxial Compressive Strength/MPa	Uniaxial Tensile Strength/MPa	Cohesion/MPa	Internal Friction Angle/°	Modulus of Elasticity/GPa	Poisson Ratio
1100	69	8.2	19.6	46	86.3	0.25
1300	65	6.8	17.5	48	90.2	0.26
1500	58	4.3	17.2	45	98.7	0.25

3.2. Structural Plane Survey and GSI Grading

The joint survey of typical engineering surrounding rocks at different depths was carried out by using manual measurement and SIROVISION three-dimensional rock mass measurement technology. There were two measurement points for each depth and a total of six measurement points. The distribution law of joints and fractures was counted at each measurement point, and the occurrence patterns of dominant joints at each measurement point were projected by the stereographic projection, as shown in Figure 4. In the figure, the arc is the projection of the dominant joint group on the equatorial plane, the square is the average vector of the dominant joint group, and the triangle is the vector of a single joint within the dominant joint group.
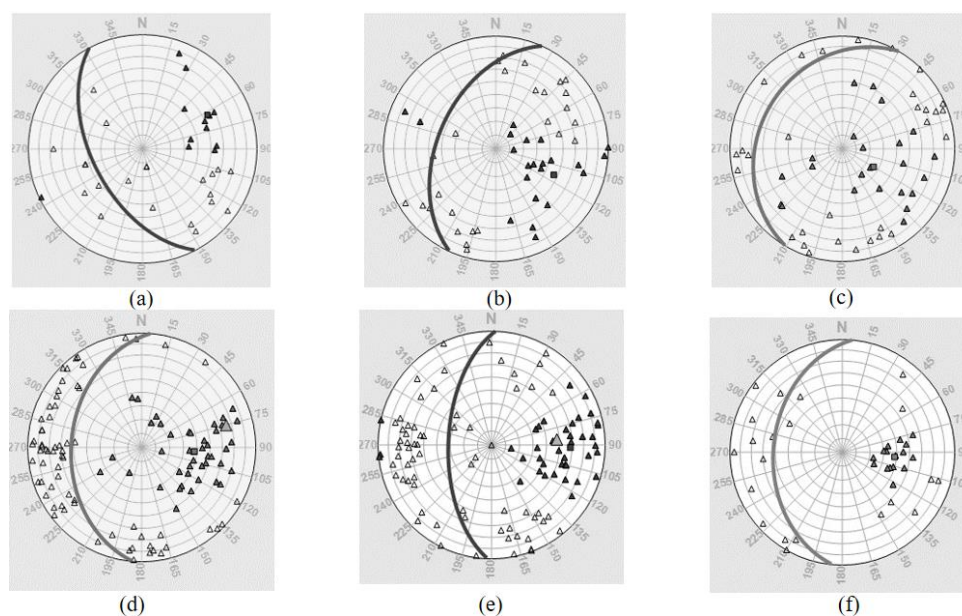
Figure 4. Stereographic projection of the occurrence of dominant joint groups at each measurement point. (**a**) point 1 (**b**) point 2 (**c**) point 3 (**d**) point 4 (**e**) point 5 (**f**) point 6.

The rock mass quality of the scanned site is graded according to the Geological Strength Index (GSI) classification method, and the results are shown in Table 2.

Table 2. Test information and joint occurrence statistics of each measurement point.

Measuring Point Number	Measuring Point Depth/m	GSI	Dominant Dip of Joint/°	Dominant Dip Angle of Joint/°	Joint Trace Length/m	Average Joint Spacing/m
1	1100	78	62.1	62.6	2.3–5.7	2.21
2	1100	52	119.6	59.2	1.3–3.4	1.38
3	1300	72	126.9	28.6	2.0–3.9	2.39
4	1300	41	92.4	49.4	0.5–2.2	0.82
5	1500	59	93.2	69.6	0.8–4.8	1.89
6	1500	44	91.9	39.9	0.9–3.3	0.94

3.3. Distribution of Ground Stress in Deep Roadway

In order to simulate the actual stress state of deep jointed rock mass under high stress, static boundary conditions should be applied in the simulation process to make the simulation as close to the actual working conditions as possible. According to the stress relief method of casing hole, the stress of the original rock at different depths of the mining area is measured, and the deep crustal stress value of the mining area is obtained, as shown in the Figure 5, Table 3.

Table 3. In situ stress distribution.

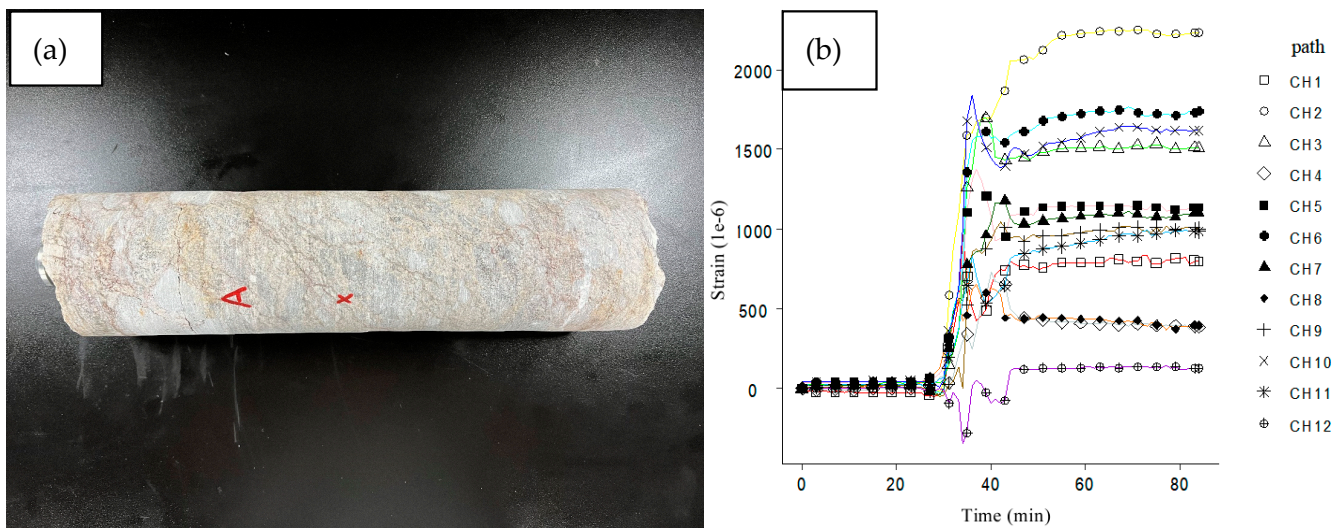| Depth/m	Maximum Principal Stress			Minimum Principal Stress			Intermediate Principal Stress		
	Value/MPa	Direction/°	Dip Angle/°	Value/MPa	Direction/°	Dip Angle/°	Value/MPa	Direction/°	Dip Angle/°
1000	25.74	330.27	29.50	16.36	76.72	26.59	22.83	203.03	48.27
1100	45.95	4.14	8.88	15.30	95.6	9.47	19.11	231.72	76.96
1300	38.05	33	−10	26.25	72	76	33.24	124	82

Figure 5. (**a**) Core; (**b**) Stress relief curve.

The regression analysis of the variation of ground stress with buried depth under different depths can be obtained:

$$\sigma_{h\text{max}} = 0.06H + 3.11 \tag{2}$$

$$\sigma_{h\text{min}} = 0.036H - 21.57 \tag{3}$$

$$\sigma_Z = 0.04H - 20.1 \tag{4}$$

where $\sigma_{h\text{max}}$, $\sigma_{h\text{min}}$, and σ_Z are, respectively, the maximum, minimum principal stress, and vertical stress, and the unit is MPa. H represents buried depth.

4. Calculation of Plastic Zone of Roadway Surrounding Rock

4.1. Calculation Results of Parameter Reduction Method

Based on the rule of parameter reduction, the mechanical parameters of rock mass with different buried depths and different GSI values were obtained. Simulation results are used in order to improve the coverage of integrity, and the field investigation in the process of different depth of surrounding rock of roadway GSI values are not covered all in interval, so on the basis of GSI scale, added interpolation GSI values 90, 80, 60, and 40 are complete, with 20 representatives constituting surrounding rock, thus representing a more complete, more broken surrounding rock.. The rock mass parameters after reduction are shown in Table 4.

The numerical model is shown in Figure 6, the size of which is 100 m × 50 m × 100 m, and the bottom boundary of the model is fixed, and the normal displacement is fixed for all four boundaries in the horizontal direction. In order to improve the calculation accuracy and efficiency as much as possible, the grid is partitioned. The closer the grids were to the surrounding roadway, the denser the grid was, and the size of grids closed to the boundary was increased appropriately. The displacement boundary conditions defined by the normal displacements of the front, and back and left surfaces were applied to the model, and the stress boundary conditions were applied according to the actual measured in situ stress data.

According to the parameters obtained by parameter reduction in Table 4, the model is assigned to simulate excavation calculation. The distribution and accumulation results of plastic zone are shown in Figure 7 and Table 5.

It can be seen from the calculation results that, with the decrease of GSI value of rock mass, the plastic zone of roadway surrounding rock gradually increases, and with the increase in roadway buried depth, the plastic zone volume also increases.

Table 4. Strength parameters of rock mass under different buried depths and different surrounding rock grades.

| Depth	GSI	Rock Uniaxial Compressive Strength/MPa	Rock Uniaxial Tensile Strength/MPa	Cohesion/MPa	Internal Friction Angle/°	Modulus of Elasticity /GPa	Poisson Ratio
	90	32.21	2.08	5.17	42.47	36.08	0.25
	78	16.92	0.66	2.91	40.18	26.22	0.25
1100	52	5.82	0.05	1.20	37.97	6.47	0.26
	40	3.60	0.01	0.81	32.18	3.44	0.28
	20	1.34	0.002	0.34	24.27	2.01	0.32
	90	30.71	1.86	4.97	42.55	37.71	0.25
	72	11.47	0.27	2.13	41.68	19.31	0.26
1300	60	7.68	0.10	1.54	38.16	10.98	0.28
	41	3.48	0.015	0.82	33.16	3.60	0.32
	20	1.30	0.002	0.32	26.28	2.10	0.35
	90	28.29	1.46	5.26	44.80	41.27	0.25
	80	10.84	0.21	2.51	43.66	21.13	0.25
1500	59	7.29	0.084	1.84	40.22	12.02	0.27
	44	3.32	0.012	0.97	38.67	3.94	0.30
	20	1.25	0.001	0.41	34.33	2.30	0.33
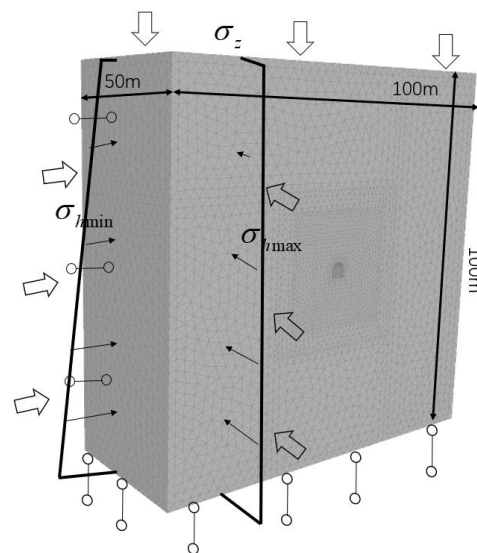
Figure 6. Numerical model.

Table 5. Plastic zone volume of roadway under different rock mass grades.

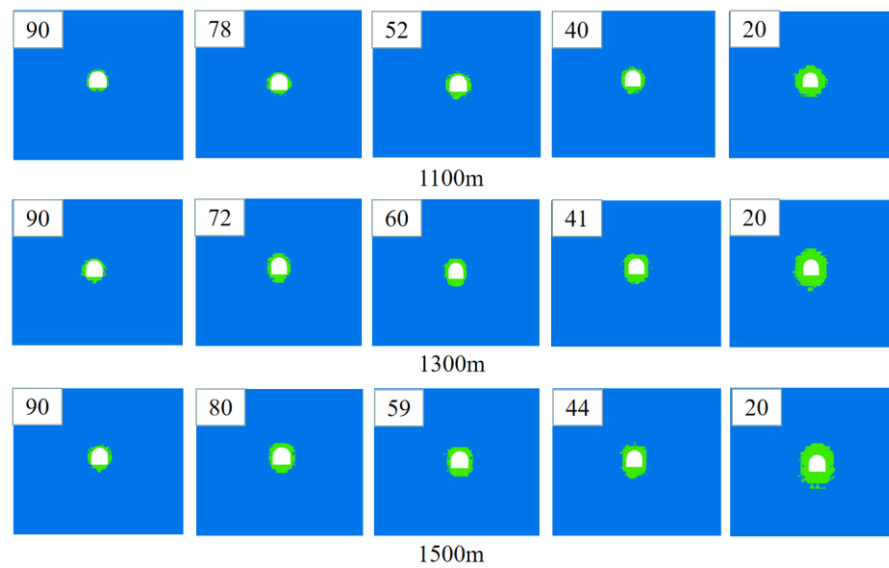| GSI	Plastic Zone Volume/m³		
	1100	1300 m	1500 m
90	491.6	551.5	552.2
80	616.9	698.8	734.3
60	905.3	1031.1	1175.1
40	1279.1	1425.9	1673.2
20	1430.4	1545.3	1814.7

Figure 7. Plastic zone distribution of surrounding rock.

4.2. Equivalent Rock Mass Technical Simulation Results

In the EQ, the size and boundary conditions of the numerical model are the same as those in the parameter reduction method, and the physical and mechanical parameters of the model are consistent with the intact rock to avoid secondary reduction. The fracture stochastic network is constructed, which is close to the actual working condition, as shown in the Figure 8. The joint formation can be controlled by the key words "dipdirlimit" and "diplimit", and the joint length is controlled by the command "size". The surrounding rocks with different GSI values are mainly reflected by the joint spacing, that is, the joint density is converted and controlled in the fish statement. For the surrounding rocks with higher GSI values without measured data, the field measured values are fitted to obtain the joint spacing under different GSI values:

$$d = 0.042 \times \text{GSI} - 1.03 \tag{5}$$
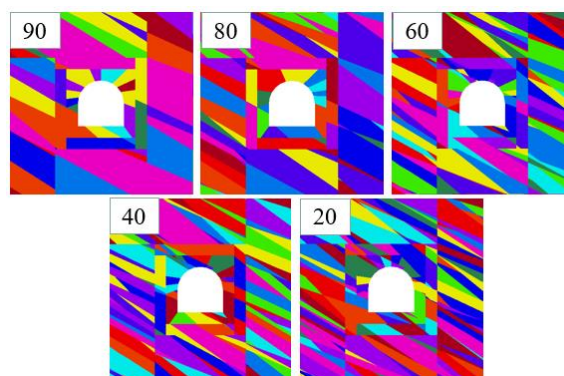
where d is the joint spacing.

Figure 8. Numerical model of equivalent rock mass with different GSI values.

It can be seen from the calculation results, as shown in the Figure 9, similar to the results obtained by the RE, with the decrease in the GSI value of rock mass, the plastic zone of roadway surrounding rock gradually increases, but the overall increase is relatively gentle, and the calculation results are smaller than that of the parameter reduction method when the quality of rock mass is poor.
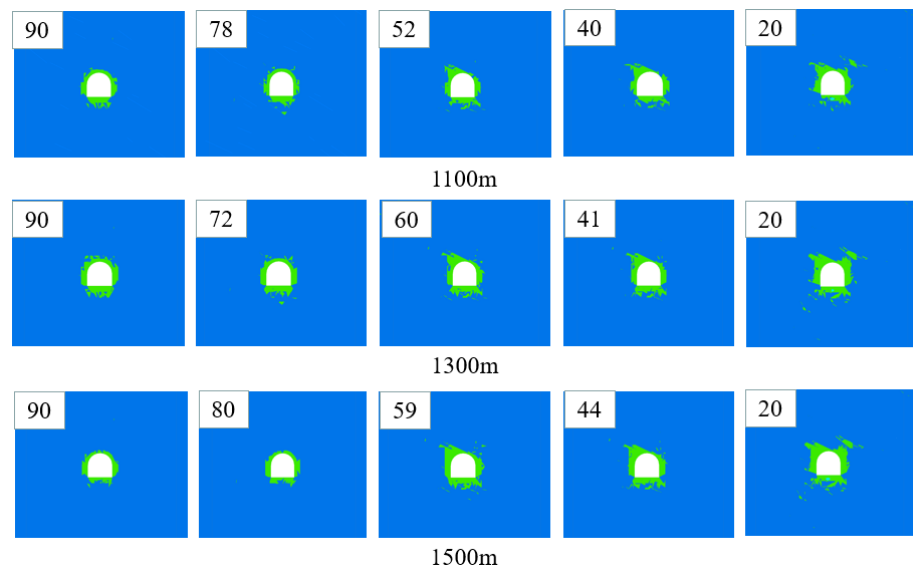
Figure 9. Plastic zone distribution of surrounding rock.

4.3. Analytical Calculation Results

Substitute the parameters in Table 4 into Equation (1). *P* is the size of the vertical stress on the upper boundary of the model. λ is the ratio of half of the sum of the horizontal principal stresses to the vertical stress, which can be calculated according to the content in Section 3.3, and R_0 is 2.5m. MATLAB software was used to calculate and draw the contour map of plastic zone boundary of Equation (1), as shown in the Figure 10, and then the plastic zone area enclosed by the contour line was integrated and multiplied by the axial length of the roadway model to obtain the volume of plastic zone, as shown in the Table 6.
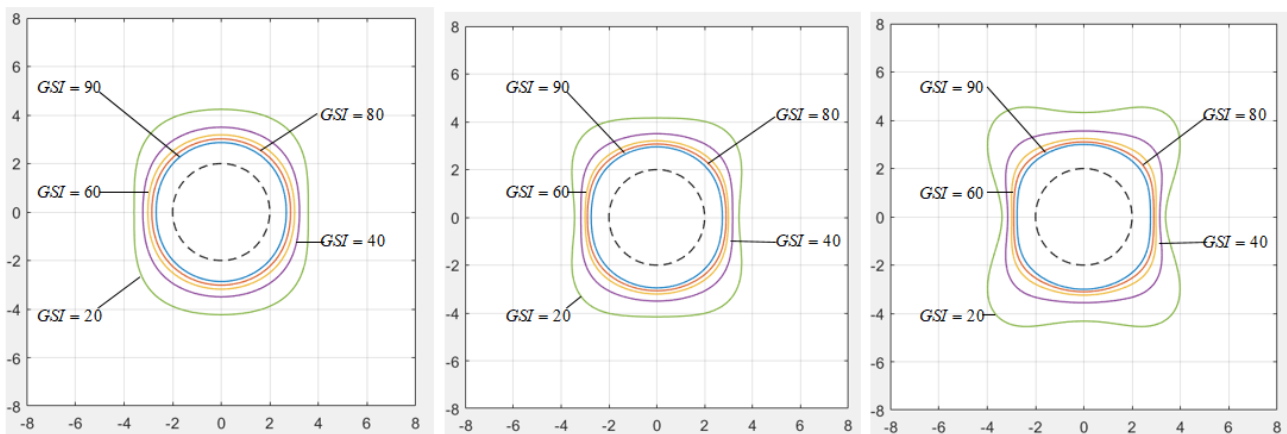

Figure 10. Plastic zone distribution of surrounding rock.

Table 6. Plastic zone volume of roadway under different rock mass grades.

GSI	Plastic Zone Volume/m³		
	1100	1300 m	1500 m
90	479.9	549.9	605.5
80	603.8	667.6	721.1
60	743.7	781.4	854.9
40	991.7	1042.2	1182.4
20	1662.1	1680.8	2135.1

5. The Site Observation of Plastic Zone in Roadway

The acoustic wave measurement method was used to measure the loosening circle at the survey site of the structural plane. The measuring device was the RSM-SY5 acoustic wave detector produced by Wuhan Zhongke Intellectual Innovation (Wuhan, China), and it is the matching one, with a double receiver probe.

The steps of field measurement are as follows. First, 7655 drilling was used to drill holes, and a measuring borehole was set at 1.7 m from the side wall of the roadway to the depth of 3 m, with a diameter of 60 mm and a depth of 3 m, and a certain downward angle was maintained to facilitate water injection, and the borehole was cleaned to remove gravel and mud. Then, the probe of the ultrasonic instrument was placed at the bottom of the hole, water was injected into the hole as a coupling agent, and the probe was pulled outward each time when it was full of water and measured every 20 cm until it reached the hole, as shown in the Figure 11.
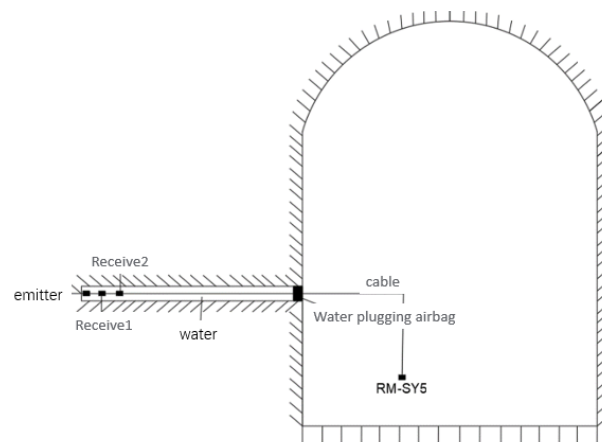

Figure 11. Schematic diagram of the field measurement in the plastic zone of the roadway.

The wave velocity values of rock mass at different depths from the surface of surrounding rock were measured by acoustic detection method, and the size range of surrounding rock loose zone was deduced according to the variation rule of the obtained wave velocity. The acoustic detection results are shown in Figure 12.
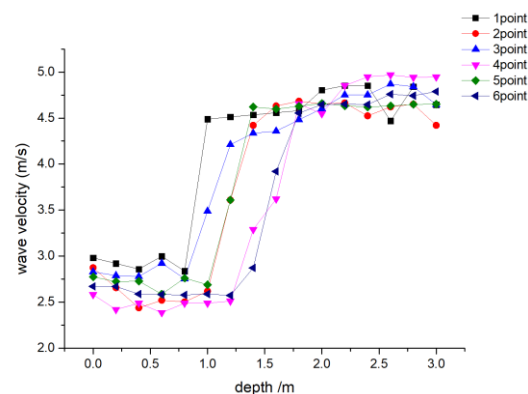

Figure 12. Acoustic wave distribution of each measuring point.

The points with obvious changes in acoustic wave velocity were identified as the boundary of the loose circle, and the areas with small wave velocity were identified as the loose circle. Then, the distance between the loose circle of measuring points 1 to 6, and the side wall of the roadway was about 1 m, 1.5 m, 1.1 m, 1.8 m, 1.5 m, and 1.9 m, respectively.

Combined with the radius of the roadway, the radius of the loose ring is converted into the radius of the plastic zone, according to the formula proposed in the literature [2].

$$R = \left(\frac{1}{1+3\alpha}\right)^{\frac{1-3\alpha}{6\alpha}} R_P \tag{6}$$

$$\alpha = \frac{\sin\varphi}{\sqrt{3(3+\sin^2\varphi)}} \tag{7}$$

where φ is the internal friction angle and R_P is the radius of the tunnel plastic zone. After conversion, the radius of the plastic zone of the roadway of the three surrounding rock grades is 3.09 m, 3.49 m, 3.09 m, 3.68 m, 3.79 m, and 3.78 m, respectively. Based on the calculation method of the cylinder volume and combined with the tunnel axial length used in the numerical model, the measured values of the plastic zone of surrounding rock in the three surrounding rock grades are 697.1, 1027.1, 697.1, 1119.5, 1302.3, and 1294.8 m^3.

6. Volume Contrast Analysis of Plastic Zone

The plastic zone volumes obtained by different methods are compared. In the Figure 13, ME represents measured method.
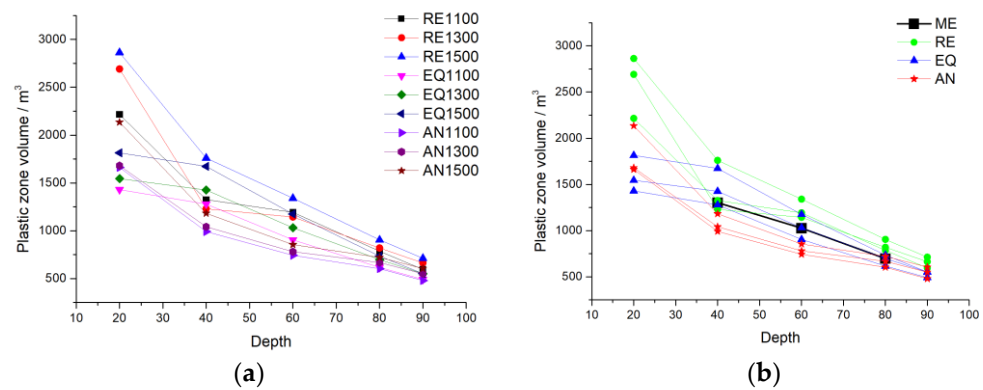

Figure 13. (**a**) Comparison between results of two methods and measured values; (**b**) Comparison between measurement and calculation.

When the GSI value of rock mass is greater than 60, the difference between the results obtained by the three calculation methods is small. When the GSI value is less than 60, the calculation results begin to show a big difference. With the decrease of GSI value, the quality of rock mass deteriorates and the degree of fragmentation increases. The change rate of the result obtained by parameter reduction method becomes larger and larger. When the GSI value is less than 40, the trend of surge occurs, and the data is generally larger than the measured value. The variation trend of the calculated results obtained by equivalent rock mass technique is the most gentle, and the error between the calculated results and the measured values is small. The results obtained by analytical method are generally smaller than the measured values.

The ratio of the difference between the calculated value and the measured value is defined as the error rate.

$$v_i = \left| \frac{V_c - V_r}{V_r} \right| \tag{8}$$

where V_c is the calculated value, V_r is the measured value, and v_i is the error rate.

The parameters required for calculation by different methods and the error rates are sorted out in the following Figure 14.
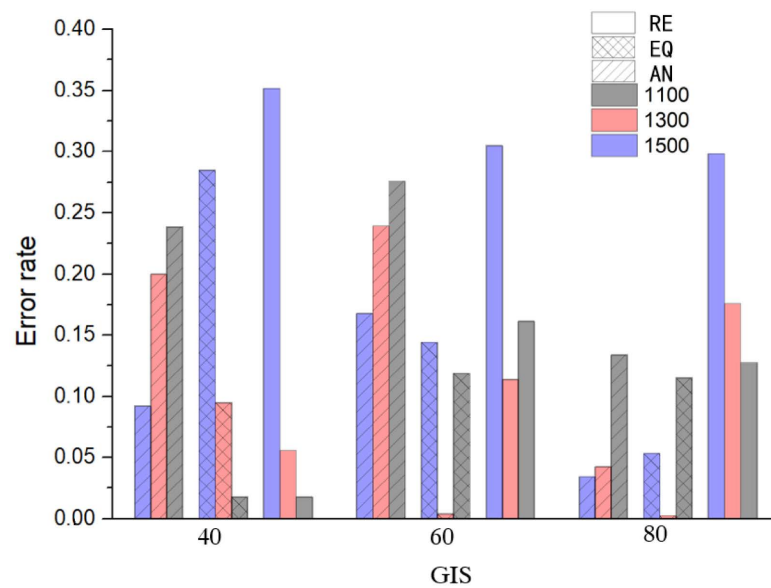
Figure 14. Error rates distribution of plastic zone under different methods, different GSI values, and different depths.

As can be seen from Figure 14, the error of RE method is larger among the three methods. The smaller the GSI value is and the deeper the depth is, the larger the error is and the more uneven the error distribution between different depths is. The error of EQ method is the smallest among the three methods. With the decrease of GSI value, the position error of deeper buried depth is gradually larger than that of shallower buried depth. The error of AN method is more uniform in depth, and the deeper the depth, the smaller the error.

The calculation parameters required by different methods are summarized in Table 7.

Table 7. Calculation parameters to be obtained by various methods.

Methods	GSI	Elasticity Modulus	Uniaxial Compressive Strength	Uniaxial Tensile Strength	Density	Internal Friction Angle	Cohesion	Side Pressure Coefficient	Frequency of Joints	Joint Trace Length	The Joint Stiffness
RE	√	√	√	√	√	√	√	√			
EQ	√	√	√	√	√	√	√	√	√	√	√
AN	√					√	√	√			

It can be seen from Table 7 that the equivalent EQ method requires the most parameters, which not only requires the physical and mechanical parameters of rocks, but also needs to pay attention to the mechanical properties of joints. The RE method requires complete rock parameters for reduction calculation, and the selection of some empirical coefficients in the reduction process is subjective. The analytical method requires the least parameters, and only some parameters of two-dimensional calculation are concerned.

7. Conclusions

(1) There is a high correlation between the plastic zone volume calculated by the three methods and the measured value, and they all increase with the decrease of GSI value, and the smaller the GSI value, the more significant the increase. When the GSI value is greater than 40, the error between the results of the three calculation methods and the measured values is small. When the GSI value is less than 40, the results obtained by the parameter reduction method and the analytical method show a more drastic increase, and the discreteness increases. The results obtained by the equivalent rock mass technique are generally close to the measured values, and the growth rate is more uniform.

(2) There is a certain error between the results obtained by the three calculation methods and the measured values. In general, the error of equivalent rock mass technology is the smallest. With the decrease of GSI value, its error rate at different depths gradually increases. The error of the parameter reduction method is the largest, and it shows great discreteness in different depths. The error of analytical method increases more evenly under different GSI values, and there is little difference between different depths.

(3) Considering the convenience of obtaining calculation parameters and the accuracy of calculation, analytical method can be used to calculate when the GSI is high, the depth is shallow, and the approximate plastic zone range needs to be determined quickly. When the GSI is high and the depth is shallow, the parameter reduction method can be used for calculation and analysis. On the premise that GSI is small, the depth is deep, and the joint mechanical properties can be obtained, and the equivalent rock mass technology can be used to calculate the plastic zone of roadway more accurately so as to guide the support and stability analysis of deep roadway.

In general, there are some errors in the three methods compared with the measured results, but the measured values are not completely accurate, so different methods can be selected to calculate the plastic zone of the roadway according to the GSI value of the surrounding rock, the distribution interval of the buried depth, and the convenience of parameter acquisition.

References

1. Zhang, Z.H.; An, L.; Wu, D.W.; Wu, C. Field detection of roadway surrounding rock loose zone and support technology of broken rock mass in jiaojia gold mine. *Met. Mine* **2019**, *12*, 56–61. [CrossRef]
2. Xu, K.; Wang, Z.J.; Meng, X.L. Research on detection technology for deep tunnel surrounding rock loose circle and numerical simulation analysis. *Rock Soil Mech.* **2013**, *34*, 464–470. [CrossRef]
3. Jing, H.W.; Li, Y.H.; Liang, J.Q.; Yu, D.C. Borehole camera technology for measuring the relaxation zone of surrounding rock: Mechanism and application. *J. China Univ. Min. Technol.* **2009**, *38*, 645–649, 669.
4. Guo, L.; Li, J.C.; Zhang, Z.C.; Chen, S.J. Research on surrounding rock loose zone of tunnel under unsymmrtrical loading with ground penetrating radar ang its application. *Chin. J. Rock Mech. Eng.* **2011**, *30*, 3009–3015.
5. Yang, K.; Wu, S.K.; Wu, Q.L.; Gao, Y.T.; Wang, Y.Q. Support optimization design of a deep-buried tunnel in consideration of the broken rock zone support. *Chin. J. Eng.* **2015**, *37*, 839–843. [CrossRef]
6. Wang, L.; Gao, Q. Elastoplastic model of damaged rock based on the strength theory. *J. Univ. Sci. Technol. Beijing* **2008**, *30*, 461–467.
7. Cai, W.; Zhu, H.; Liang, W.; Wang, X.; Su, C.; Wei, X. A post-peak dilatancy model for soft rock and its application in deep tunnel excavation. *J. Rock Mech. Geotech. Eng.* **2022**, *in press*. [CrossRef]
8. Cai, W.Q.; Zhu, H.H.; Liang, W.H. Three-dimensional stress rotation and control mechanism of deep tunneling incorporating generalized Zhang–Zhu strength-based forward analysis. *Eng. Geol.* **2022**, *308*, 106806. [CrossRef]
9. Cai, W.; Zhu, H.; Liang, W.; Vu, B.; Su, C.; Zhang, K.; Wang, X. Three-dimensional forward analysis and real-time design of deep tunneling based on digital in-situ testing. *Int. J. Mech. Sci.* **2022**, *226*, 107385. [CrossRef]
10. Xiao, M.; Zhang, Y.T.; Chen, J.T.; Tian, H. Numerical analysis of excavation damaged zone of underground caverns include by excavation blasting. *Rock Soil Mech.* **2010**, *31*, 2613–2618. [CrossRef]
11. Zhou, Z.H.; Yang, L.D.; Duan, Y. Numerical simulation of the broken zone in soft rock roads. *China Min. Mag.* **2009**, *18*, 97–99.
12. Xiong, L.X.; Yang, D.L. Stress evolution of deep cavern included by excavating. *J. Cent. South Univ. (Sci. Technol.)* **2009**, *40*, 236–242. [CrossRef]
13. Zuo, S.Y.; Xiao, M.; Xu, J.K. Numerical simulation of dynamic damage effect of surrounding rock for tunnels by blasting excavation. *Rock Soil Mech.* **2011**, *32*, 3171–3176, 3184. [CrossRef]

14. Sun, L.H.; Ji, H.G.; Zeng, P.; Jiang, H. Variability characteristics simulation of roadway plastic zone in different side pressure coefficients. *Saf. Coal Mines* **2015**, *46*, 227–230. [CrossRef]
15. Xu, W.Y.; Zhang, G.K. Study on orthotropic equivalent strength parameters of jointed rock mass. *Chin. J. Geotech. Eng.* **2007**, *29*, 806–810.
16. Fan, W.C.; Cao, P. Degradation of joint surface morphology, shear behavior and closure characteristics during cyclic loading. *J. Cent. South Univ.* **2018**, *25*, 653–661. [CrossRef]
17. Liu, C.; Bai, S.W. Fuzzy mathematics method for analysis of the weathering degree of rocks. *Chin. J. Rock Mech. Eng.* **2005**, *26*, 252–256.
18. Hoek, E.; Brown, E.T. The Hoek–Brown failure criterion and GSI—2018 edition. *J. Rock Mech. Geotech. Eng.* **2019**, *11*, 445–463. [CrossRef]
19. Fraldi, M.; Cavuoto, R.; Cutolo, A.; Guarracino, F. Stability of tunnels according to depth and variability of rock mass parameters. *Int. J. Rock Mech. Min. Sci.* **2019**, *119*, 222–229. [CrossRef]
20. Fraldi, M.; Guarracino, F. Limit analysis of progressive tunnel failure of tunnels in Hoek-Brown rock masses. *Int. J. Rock Mech. Min. Sci.* **2012**, *50*, 170–173. [CrossRef]
21. Fraldi, M.; Guarracino, F. Evaluation of impending collapse in circular tunnels by analytical and numerical approaches. *Tunn. Undergr. Space Technol.* **2011**, *26*, 507–516. [CrossRef]
22. Gao, Y.T.; Fan, G.L.; Wu, S.C.; Han, H.L.; Gao, L.L.; Zhou, Y. Stability analysis of tunnel surrounding rock based on different strength reduction paths. *J. Univ. Sci. Technol. Beijing* **2013**, *35*, 393–401.
23. Hu, S.M.; Hu, X.W. Estimation of rock mass parameters based on quantitative GSI system and Hoke-Brown criterion. *Rock Soil Mech.* **2011**, *32*, 861–866. [CrossRef]
24. Su, Y.H.; Feng, L.Z.; Li, Z.Y.; Zhao, M. Quantification of elements for geological strength index in Hoke-Brown criterion. *Chin. J. Rock Mech. Eng.* **2009**, *28*, 679–686.
25. Wu, S.C.; Zhou, Y.; Gao, Y.T.; Misra, A. Research on construction method of stochastic joints 3d-network model of equivalent rock mass. *Chin. J. Rock Mech. Eng.* **2012**, *31*, 3082–3090.
26. Zhou, Y.; Wu, S.C.; Wang, L.; Yan, Q.; Zhao, W.; Zhang, X.P. Application of equivalent rock mass technique to mesoscopic analysis of fracture mechanism of rock specimen containing two intermittent joint. *Rock Soil Mech.* **2013**, *34*, 2801–2809. [CrossRef]
27. Yang, Z.M.; Gao, Y.T.; Wu, S.C.; Chengzi, B.; Jin, A. Study of influence of joint parameters on rock mass strength based on equivalent rock mass technology. *J. China Univ. Min. Technol.* **2018**, *47*, 979–986. [CrossRef]
28. Zhu, W.C.; Zhang, M.S.; Zhang, H.X.; Guo, X.Q.; Guan, K. Numerical simulation for determining the size of representative element volume (REV) of jointed rock mass. *Chin. J. Geotech. Eng.* **2013**, *35*, 1121–1127.
29. Wu, S.C.; Zhou, Y.; Gao, L.L.; Zhang, X.P. Application of equivalent rock mass technique to rock mass engineering. *Chin. J. Rock Mech. Eng.* **2010**, *29*, 1435–1441.
30. Wang, X.M.; Zheng, Y.H. Review of advances in investigation of representative elementary volume and scale effect of fractured rock masses. *Rock Soil Mech.* **2015**, *36*, 3456–3464.
31. Zhao, Z.Q. Study on Deformation Failure Mechanism and Control Method of Surrounding Rock in Large Deformation Mining Roadway. Ph.D. Thesis, China University of Mining & Technology, Beijing, China, 2014.
32. Yuan, C. Study on Deformation Failure Mechanism and Stability Control Principle of Deep Roadway Surrounding Rock. Ph.D. Thesis, China University of Mining & Technology, Beijing, China, 2014.